

**Reorganization of a dense granular assembly: The unjamming response function**

Évelyne Kolb,\* Jean Cviklinski,\* José Lanuza,\* Philippe Claudin,\* and Éric Clément\*

*Laboratoire des Milieux Désordonnés et Hétérogènes, UMR 7603, Université Pierre et Marie Curie, Boîte 86, 4 Place Jussieu, 75252 Paris Cedex 05, France*

(Received 4 August 2003; published 30 March 2004)

We investigate the mechanical properties of a static dense granular assembly in response to a local forcing. To this end, a small cyclic displacement is applied on a grain in the bulk of a two-dimensional disordered packing under gravity and the displacement fields are monitored. We evidence a dominant long range radial response in the upper half part above the solicitation and after a large number of cycles the response is “quasireversible” with a remanent dissipation field exhibiting long range streams and vortexlike symmetry.

DOI: 10.1103/PhysRevE.69.031306

PACS number(s): 45.70.-n, 83.50.-v

It is always striking that apparently different cellular materials like foams, emulsions, or granular systems share in common many rheological properties [1]. All these systems can flow like fluids when a sufficiently high external stress is applied but jam into an amorphous rigid state below a critical yield stress. This jamming transition is associated with a slowdown of the dynamics which led Liu and Nagel [1] to propose an analogy between the process of jamming and the glass transition for glass-forming liquids. Although the nature of this jamming transition is still unclear experimentally [2,3], several theoretical attempts were made to adapt the concepts of equilibrium thermodynamics to athermal systems out of equilibrium [4–6]. For packing made of grains with a size larger than few microns, thermal fluctuations are too small to allow a free exploration of the phase space and grains are trapped into metastable configurations. The system cannot evolve until an external mechanical perturbation like shear or vibration is applied, which allows grains to overcome energy barriers and triggers structural rearrangements. In this case, the free volume and configurations accessible to each grain are capital notions that were used to define the new concept of “effective temperature” [4]. Recently it was proposed that this notion could account for the transport properties in the vicinity of a jammed state [7]. However besides this large number of theoretical and numerical works there are only few experiments connecting the motion at the grain level to the macroscopic mechanical behavior [8]. It appears that there is a crucial need for understanding the connection between the local geometrical properties and the possible motion of a grain since structural rearrangements, and therefore displacement fields, are the key for understanding the rheology of dense systems.

On the other hand, there is still a debate to understand the elastoplastic behavior of amorphous materials [9–12]. Recent experiments on the response of a granular pile to a small force perturbation revealed an elasticlike behavior, which is very sensitive to the preparation, i.e., to the microscopic texture [13]. Similar conclusions were drawn in the context of sound propagation [14]. However, at this stage it is not en-

tirely clear which features of the texture (such as coordination number, contact distribution, various fabric tensors) are useful to build relevant macroscopic constitutive relations [15]. When the external drive increases an irreversible yield occurs that is usually described by a plasticity theory. Yet the study of the early stages of plasticity is of crucial interest for a better understanding of yield properties and the elucidation of strain localization (shear bands). Recent theoretical attempts were made to explain global plastic deformations from a modeling of local structural rearrangements named “shear transformation zone.” This approach was first introduced to account for the onset of plasticity in amorphous solids [11] but was extended to granular materials [16].

In this paper, we present a conceptually simple experiment which aims to study the response of a dense disordered granular media to a small perturbation induced by the displacement of a grain-scale intruder. The forces applied to the intruder grain are large enough to unjam this initially static packing but the driving is slow enough to stay in the *quasi-static* regime. Deformations induced by the local perturbation are small (less than  $10^{-2}$ ) and so we are rather far from a fully developed plasticity regime that would be induced, for example, by a moving rod [17]. We propose a path of study for the jammed state by monitoring the displacement fields in response to a localized cyclic perturbation that brings the system above the jamming transition. We call it the “unjamming response” function which should be a characteristic feature of the packing configurations and of its reorganization properties. Note that, very recently, similar displacement response experiments have been performed by Moukarzel *et al.* [18].

The typical displacements induced by the perturbation are small at the scale of a grain: we observe a range of displacements between  $1/2000$  and  $1/3$  of a grain size  $d$  but these are still very large compared to the local displacements induced by the granular contact deformations. A simple order of magnitude calculation shows that grains can be considered as rigid, since for the metallic grains we use and the load experienced by the packing under gravity, elastic displacements at contacts are as small as  $10^{-8}d$ . This huge separation of scales shows that we are probing the response of the granular assembly solely due to grain reorganizations. It corresponds either to contact opening/closing or to a change of contact direction (rolling contact). Under gravity these processes

---

\*Present address: Laboratoire de Physique et Mécanique des Milieux Hétérogènes, ESPCI, 10 rue Vauquelin, 75231 Paris Cedex 05, France.

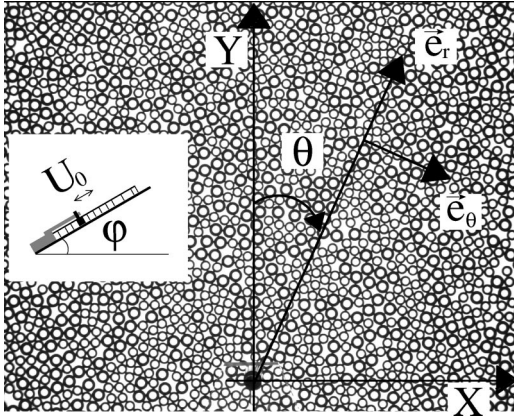


FIG. 1. Top view of the piling (inset: sketch of the experimental setup viewed from the side).

may be partially reversible and depend in a very sensible way on the packing geometrical properties (texture, density) and on how far we are from the jamming transition. This sensitivity can be seen as the hallmark of the “fragile” character of granular assemblies and the questions raised to understand this relation are important to obtain a fully consistent picture of condensed jammed phases as described for example by O’Hern *et al.* [19].

A sketch of the experimental setup is shown in Fig. 1, inset. We prepare disordered two-dimensional (2D) packings of brass hollow cylinders by mixing small (diameter  $d_1 = 4$  mm) and big ones ( $d_2 = 5$  mm) in order to avoid macroscopic crystallization. We chose to have the total mass of small cylinders to be equal to that of the big ones, so that their numbers are, respectively, in proportion of 7 to 4. This geometry allows a precise monitoring of the displacements for each grain in the visualization field. All cylinders have a 3 mm height and lie on a low frictional glass plane. The lateral and bottom walls are made of plexiglas and delimits a rectangular frame of  $L = 26.8$  cm  $\approx 54d_2$  width and an adjustable height of typically  $H = 34.4$  cm  $\approx 70d_2$ . The bottom plane can be tilted at an angle  $\phi = 33^\circ$  such as to control the confinement pressure inside the granular material by an effective gravity field  $g \sin \phi$ . The angle  $\phi$  value is larger than the static Coulomb angle of friction between the grains and the glass plate. The intruder is a big grain of diameter  $d_2$  located in the median part of the container at a 21.2 cm (i.e.  $\approx 42d_2$ ) depth from the upper free surface. It is attached to a rigid arm in plexiglas moved by a translation stage and a stepping motor driven by a computer, so that the intruder motion is characterized by cycles of displacement along the median axis  $Y$  of the container. In this report the intruder is moving up then down in a quasistatic way at a velocity of  $156 \mu\text{m/s}$  separated by rest periods of 9 s. The intruder displacement value  $U_0$  is only a fraction of a grain diameter ( $U_0 = 1.25$  mm). A high resolution charge-coupled device (CCD) camera ( $1280 \times 1024$  pixels<sup>2</sup>) is fixed above the experimental setup with its plane parallel to the tilted plane which is homogeneously illuminated from behind. The image frame is centered slightly above the intruder and covers a zone of area  $39d_2 \times 31d_2$ ; see Fig. 1. The camera is triggered by a signal coming from the motor which allows the capture

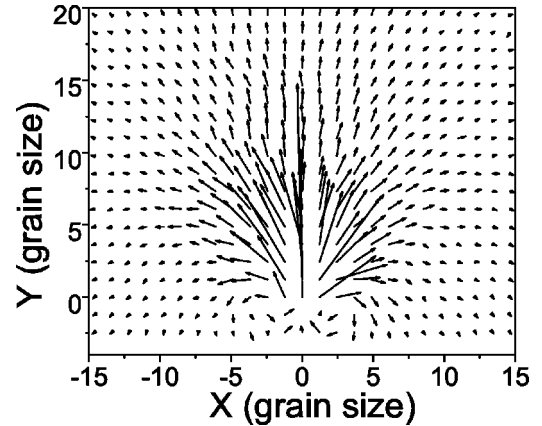


FIG. 2. Averaged displacement field for the second upward motion of the intruder ( $n=2, i=3$ ). Note that all displacements are magnified by a factor of 70. The intruder is located at  $X=Y=0$ .

of an image in the rest phase one second before each intruder displacement. In the following, we use the notation  $i$  for the index corresponding to the  $i$ th image just before the  $i$ th displacement (upwards or downwards) and  $n$  for the cycle number with  $n = \text{int}[(i+1)/2]$ . The center of each grain is determined with precision using the computation of the correlation between an image of the packing and two reference images corresponding to both grain types ( $d_1$  or  $d_2$ ). We obtain, for each image, the locations of more than a thousand grains with a resolution down to 0.05 pixels. The displacements of each single grain in response to the intruder motion is determined with a precision of less than  $10 \mu\text{m}$ .

To compute the averaged displacement fields we first coarse grain individual grain displacements in little cells of typical size  $1.2d_2 \times 1.2d_2$  regularly located in the Cartesian coordinates ( $O, X, Y$ ) reference frame; see Fig. 1. We then use an ensemble average. To this end, 16 equivalent experiments were performed by fixing the initial compacity at a value  $\phi = 0.760 \pm 0.005$  and using the same preparation method for each packing: the initial grain configuration is randomly mixed in the horizontal position—the packing lying on the bottom plane and then slowly inclined at  $\phi$ . We directly tested that packing fraction does not vary by more than 0.5% during each experiment. The final precision for the mean displacement per cell is less than  $2 \mu\text{m}$ . Hence, we obtain for each cycle  $n$  the displacement fields  $\vec{u}_n^\uparrow$  in response to the upward intruder motion and  $\vec{u}_n^\downarrow$  in response to the subsequent downward motion. The irreversible or plastic displacement field  $\vec{a}_n$  is defined through the relation:  $\vec{u}_n^\downarrow = -\vec{u}_n^\uparrow + \vec{a}_n$ .

In Fig. 2, we show the ensemble average and coarse-grained displacement field obtained after the second upward motion of the intruder (cycle  $n=2$ , displacement  $i=3$ ). We clearly note that the granular motion is not localized in the vicinity of the intruder and that this small perturbation of only one third of a grain diameter produces a far field effect. The presence of two displacement rolls is observed near the intruder. They are located symmetrically on each side of the intruder but turn in opposite directions. Besides this near field effect, the main response principally occurs above the

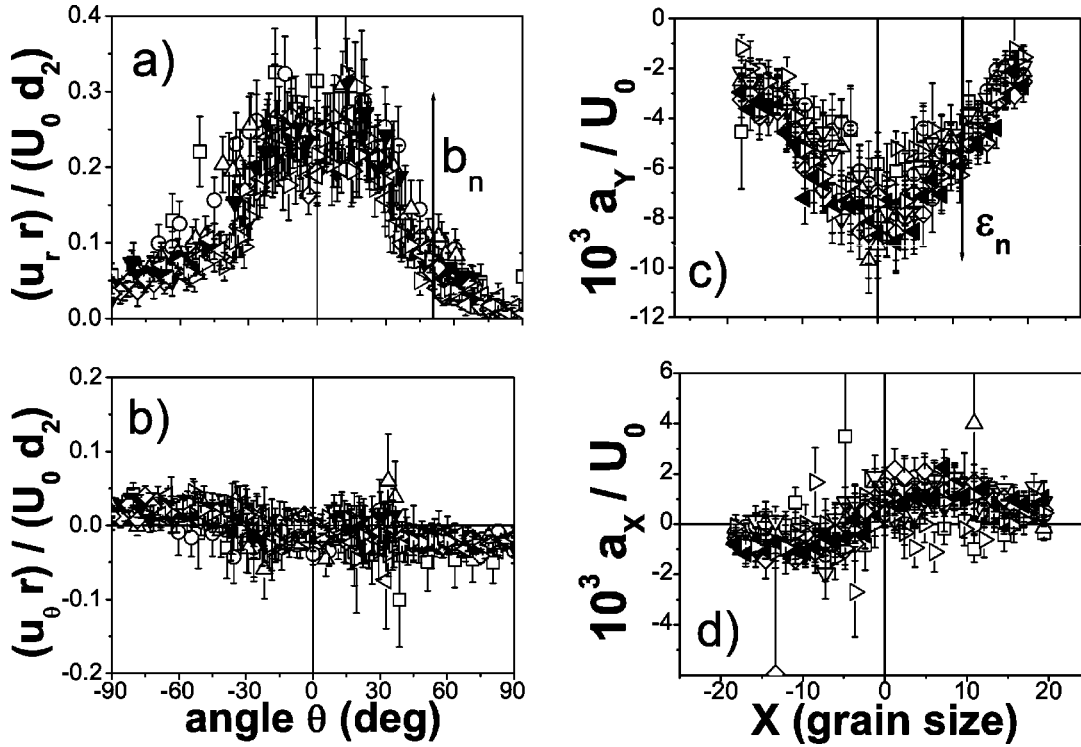


FIG. 3. (a) and (b) Mean rescaled response functions in polar coordinates  $ru_r$  and  $ru_\theta$  for the upward motion  $i=17$  ( $n=9$ ) as a function of  $\theta$ . This data collapse has been obtained with radial distances ranging from  $7.4d_2$  to  $21.8d_2$ , represented by different symbols, e.g.,  $\blacktriangledown$  for  $r=15.8d_2$ . (c) and (d) Vertical and horizontal components of the irreversible displacement field  $\vec{a}$  for cycle  $n=9$  in Cartesian coordinates as a function of  $X$ . The horizontal span corresponds to the whole cell width. Here the data correspond to  $Y$  between  $14.5d_2$  and  $26.7d_2$ , e.g.,  $Y=24.2d_2$  is  $\blacktriangleleft$ . Rescaling factors are indicated on the axis legends. The quantities  $b_n$  and  $\epsilon_n$  are the maxima of the mean profiles (a) and (c), respectively.

intruder with displacement vectors that tend to align along the radial directions from the intruder. In Figs. 3(a) and 3(b) we display a typical response to the  $n=9$ th upward motion ( $i=17$ ) in polar coordinates  $(0, r, \theta)$ . By defining  $\vec{u}_n^\dagger = u_{n,r}\vec{e}_r + u_{n,\theta}\vec{e}_\theta$ , we display the rescaled quantities:  $ru_{n,r}$  and  $ru_{n,\theta}$  as a function of the angle  $\theta$ . The collapse of the data onto the same curve (within experimental uncertainties) at distances far enough from the intruder ( $r \geq 6d_2$ ) shows that we can extract a *dominant* term for the far field displacement of the type:

$$\vec{u}_n^\dagger \simeq b_n U_0 d_2 \frac{f(\theta)}{r} \vec{e}_r. \quad (1)$$

The parameter  $b_n$  is a dimensionless decreasing function of the cycle number  $n$  (see further) and  $f(\theta)$  is an even function of  $\theta$  with  $f(0)=1$ . Note that we could not observe any significant shape variation of the function  $f(\theta)$  with  $n$ . The preceding formula holds for the zone above the intruder, i.e.,  $-90^\circ \leq \theta \leq 90^\circ$ , as the decay of the response below the intruder is much faster than  $1/r$ . According to Eq. (1) the projection  $u_{n,Y}(X, Y)$  of  $\vec{u}_n^\dagger$  along  $\vec{e}_Y$  should be maximal in  $X=0$  for a given vertical distance  $Y$  from the intruder, leading to  $u_{n,Ymax}(Y) \simeq b_n U_0 d_2 / Y$ . Simple integration of  $u_{n,Y}$  along the  $X$  axis shows that the quantity  $b_n U_0 d_2$  is proportional to the effective area displaced by the intruder on the horizontal

line seen at a remote vertical distance  $Y$ . Thus, in this interpretation, parameter  $b_n$  can be seen as an “effective transmission” parameter or a “displacement impedance” connecting the externally driven motion of the intruder to the granular reorganizations in the bulk. A good determination of  $b_n$  can be inferred from average of the experimental quantity  $\beta_n = Yu_{n,Ymax} / (U_0 d_2)$  over values of  $Y$  in between  $6d_2$  and  $27d_2$ .

Now we study the behavior of the irreversible field  $\vec{a}_n$  for the transient part of the response. After few cycles its amplitude is relatively small: one tenth or less of the displacement field magnitude. In Figs. 3(c) and 3(d), we display the Cartesian coordinates of  $\vec{a}_n = a_{n,X}\vec{e}_X + a_{n,Y}\vec{e}_Y$  for a cycle number  $n=9$  and for different heights far from intruder level. We observe a striking feature: the dominant part of the field has an amplitude almost independent of the vertical distance and its influence spans the whole width of the container ( $27d_2$  on each side). It can be described as a quasivertical columnar flow with a linear decay of its amplitude out of the median axis, as to first order, the shape of the field is triangular with a maximum value  $a_{n,max}$  in  $X=0$ . The measurement error bars prevent more precise determination of the field shape. We also note that the horizontal part of the field  $a_{n,X}$  is not exactly zero and could actually show a slight tendency to point outwards the median line but we are at the limit of the signal over noise ratio to go further in the analysis.

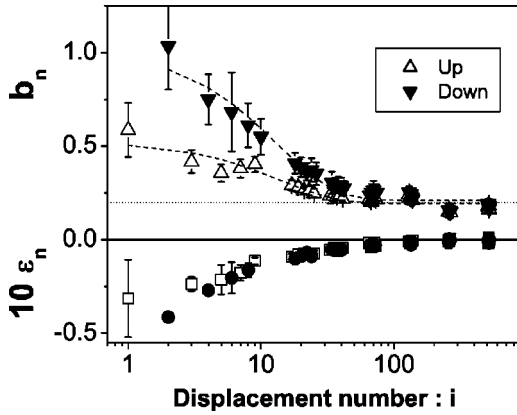


FIG. 4. Evolution of the plateau value  $b_n$  (upper part) and the rescaled irreversible component  $\epsilon_n \equiv a_{n,max}/U_0$  (bottom part) vs the displacement number  $i$  or equivalently  $n$  with  $n = \text{int}[(i+1)/2]$ . The value  $a_{n,max}$  is computed as the mean of the maximum vertical component of the irreversible field  $\vec{a}_n$ . The definition of  $b_n$  initially introduced for upward motions of the intruder is extended to downward motions.

Both reversible and irreversible displacement fields evolve with the number of cycles. On the upper part of Fig. 4, we display the evolution of the values  $b_n$  as a function of the displacement number  $i$ . The error bar on  $b_n$  is a witness of the dispersion of the quantity  $\beta_n$ : it is larger for the first two cycles where there is a departure from the scaling proposed in Eq. (1). From Fig. 4 we observe a quasiexponential relaxation to a limiting value  $b_n = 0.19 \pm 0.01$  which is three times smaller than the original one. This decrease of  $b_n$  can be interpreted as a progressive screening of the perturbation and is due to a local arching effect that takes place at a distance of few grains around the intruder. These observations seem to validate, at least in the limit of experimental uncertainties, the interpretation of  $b_n$  as a displacement impedance. The screening due to this arching effect progressively ceases to vary for a number of cycles larger than few tens as evidenced by the steady saturation of the  $b_n$  values for  $n \geq 30$ . In parallel (Fig. 4, bottom part), we monitor the mean maximal amplitude  $a_{n,max}$  of the irreversible component  $a_{n,Y}$ . We observe its decay to zero for  $i \geq 60$ , i.e.,  $n \geq 30$  which corresponds to the onset of a quasireversible response observed from the curve  $b_n(i)$ .

In the quasireversible regime ranging from  $n=30$  up to  $n=262$  for the longest experiments we did, we could not observe any sensible variation of the ensemble average fields ( $\vec{u}_n^I$  or  $\vec{a}_n$ ) and compacity. On the other hand, a closer look at *each individual experimental realization* of the irreversible displacement field shows a very striking feature; see Fig. 5. The irreversible displacement field has radically changed its symmetry: coherent streams and vortexlike structures appear in the whole packing. What is not clear yet is whether this structuring will lead to a further slower evolution of the packing or whether it corresponds to some steady-state feature, i.e., a remanent steady dissipation field. The long range coherent structures found in many different situations are, in our opinion, of a central importance since they could carry

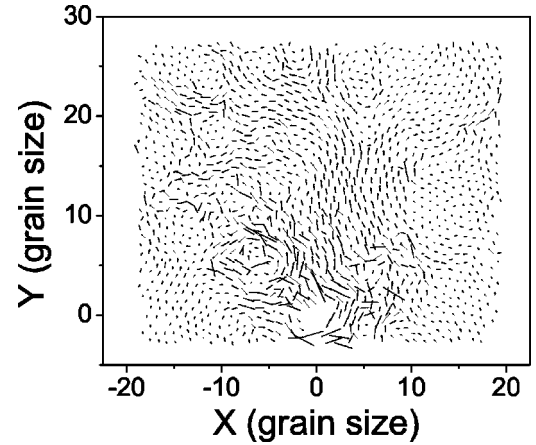


FIG. 5. Irreversible displacement field for a given experiment. The arrows represent the cumulative displacement of each grain between the images  $i=129$  and  $i=513$  (magnified by a factor of 20).

some universal features characterizing the collective dissipation modes of condensed jammed phases.

In conclusion, we propose the experimental determination of the “unjammed response” i.e., the reorganization field due to a localized cyclic displacement experienced by a packing of hard grains under gravity. We use a small perturbation such as to investigate intermediate values of deformations which are large compared to the deformations at granular contacts but small compared with usual experiments where a plastic deformation field is fully developed. The response to an upward perturbation can be separated into three distinct parts. Far from the intruder we observe a dominant radial displacement field whose amplitude scales as the inverse of the distance to the perturbation. Close to the perturbation we observe displacement rolls on both sides as well as a vault forming in the immediate surrounding of the intruder. In the part below the intruder the displacement decays rapidly to zero. A local arching effect progressively screens the perturbation as seen far from the intruder and is accompanied by an irreversible field shaped as a quasivertical columnar flow. This irreversible downward flow is too small to induce noticeable changes of compacity but is sufficient to modify the subsequent mechanical response. Thus the granular material can be seen as an autoadaptive material screening the exerted perturbation. Once this flow ceases, the response is quasireversible but on each realization, we still observe a remanent irreversibility flow spanning the whole container and characterized by a different symmetry: vortexlike structures and coherent long range streams. These vortexlike structures remind strongly what was observed recently in simulations for the nonaffine components of the elastic field in amorphous media [12] and also for the particle displacement fluctuations in a quasistatically sheared granular flow [20]. The question whether these features are linked to the 2D aspect of the studied systems, and that 3D granular assemblies may behave differently has to be investigated. In the future we plan to compare these experimental data with theoretical predictions, e.g., elastic calculations

such as those computed in Ref. [12] or [21] in the context of 2D amorphous media. At last, it would be interesting to monitor the change of the unjamming response function with respect to initial compacity and/or to texture parameters in association with force measurements. This systematic study could bring some crucial informations on the nature of the jamming/unjamming transition.

We thank J.-L. Barrat, R. P. Behringer, R. Bouamrane, J.-C. Géminard, J. Goddard, I. Goldhirsch, J. E. S. Socolar, A. Tanguy, and J. P. Wittmer for fruitful interactions and comments. E.K. also thanks J. Treiner for his kind support. Finally, we are grateful to A. Poirier and L. Baouze for their experimental contribution during their undergraduate training period.

- 
- [1] A.J. Liu and S.R. Nagel, *Nature (London)* **396**, 21 (1998).  
 [2] G. D'Anna and G. Grémaud, *Nature (London)* **413**, 407 (2001).  
 [3] F. da Cruz, F. Chevoir, D. Bonn, and P. Coussot, *Phys. Rev. E* **66**, 051305 (2002).  
 [4] S.F. Edwards and R.B.S. Oakeshott, *Physica A* **157**, 1080 (1989).  
 [5] I.K. Ono, C.S. O'Hern, D.J. Durian, S.A. Langer, A.J. Liu, and S.R. Nagel, *Phys. Rev. Lett.* **89**, 095703 (2002).  
 [6] A. Fierro, M. Nicodemi, and A. Coniglio, *Phys. Rev. E* **66**, 061301 (2002).  
 [7] H.A. Makse and J. Kurchan, *Nature (London)* **415**, 614 (2002).  
 [8] O. Pouliquen, M. Belzons, and M. Nicolas, *Phys. Rev. Lett.* **91**, 014301 (2003).  
 [9] I. Goldhirsch and C. Goldenberg, *Eur. Phys. J. E* **9**, 245 (2002).  
 [10] C. Gay and R. da Silveira, e-print cond-mat/0208155.  
 [11] M.L. Falk and J.S. Langer, *Phys. Rev. E* **57**, 7192 (1998).  
 [12] J.P. Wittmer, A. Tanguy, J.-L. Barrat, and L.J. Lewis, *Europhys. Lett.* **57**, 423 (2002); A. Tanguy, J.P. Wittmer, F. Leonforte, and J.-L. Barrat, *Phys. Rev. B* **66**, 174205 (2002); F. Leonforte, A. Tanguy, J.P. Wittmer, and J.-L. Barrat, e-print cond-mat/0309623.  
 [13] G. Reydellet and E. Clément, *Phys. Rev. Lett.* **86**, 3308 (2001); D. Serero, G. Reydellet, P. Claudin, E. Clément, and D. Levine, *Eur. Phys. J. E* **6**, 169 (2001); J. Geng, D. Howell, E. Longhi, R.P. Behringer, G. Reydellet, L. Vanel, E. Clément, and S. Luding, *Phys. Rev. Lett.* **87**, 035506 (2001).  
 [14] B. Gilles and C. Coste, *Phys. Rev. Lett.* **90**, 174302 (2003); B. Velický and C. Caroli, *Phys. Rev. E* **65**, 021307 (2002).  
 [15] H.A. Makse, D.L. Johnson, and L.M. Schwartz, *Phys. Rev. Lett.* **84**, 4160 (2000).  
 [16] A. Lemaître, *Phys. Rev. Lett.* **89**, 195503 (2002).  
 [17] I. Albert, J.G. Sample, A.J. Morss, S. Rajagopalan, A.-L. Barabási, and P. Schiffer, *Phys. Rev. E* **64**, 061303 (2001).  
 [18] C.F. Moukarzel, H. Pacheco-Martínez, J.C. Ruiz-Suarez, and A.M. Viales, e-print cond-mat/0308240.  
 [19] C.S. O'Hern, S.A. Langer, A.J. Liu, and S.R. Nagel, *Phys. Rev. Lett.* **86**, 111 (2001); **88**, 075507 (2002).  
 [20] F. Radjai and S. Roux, *Phys. Rev. Lett.* **89**, 064302 (2002).  
 [21] S. Courty, B. Dollet, K. Kassner, A. Renault, and F. Graner, *Eur. Phys. J. E* **11**, 53 (2003).